Electrochemistry Communications 132 (2021) 107139

Contents lists available at ScienceDirect

Electrochemistry Communications

journal homepage: www.elsevier.com/locate/elecom

Electrodeposition of mirror surface β-W films in molten CsF–CsCl–WO_3

Xianduo Meng, Yutaro Norikawa, Toshiyuki Nohira [*]

Institute of Advanced Energy, Kyoto University, Gokasho Uji, Kyoto 611-0011, Japan

ARTICLE INFO

Keywords:
Tungsten films
β-Tungsten
Electrodeposition
Molten salt
CsF–CsCl

ABSTRACT

In this study we report, for the first time, a thick β-W film with a mirror-like surface prepared through electrodeposition involving a CsF–CsCl eutectic melt combined with 2.0 mol% of WO_3 at 773 K. A smooth-surfaced β-W film with a thickness of 13 μm was obtained when galvanostatic electrolysis was performed at − 4 mA cm^{-2}. X-ray diffraction analysis revealed that the obtained β-W films have a strong preferred orientation along the {1 1 1} plane, which becomes stronger with decreasing current density. Surface and cross-sectional morphologies observed through scanning electron microscopy indicated that increasing the current density caused the growth of the electrodeposit to change from the field-oriented texture type to the unoriented dispersion type, in accordance with Fischer's classification of electrodeposition. To the best of our knowledge, this is the first time that mirror-like metal films have been electrodeposited in a high temperature molten salt, not only for tungsten but for any metal.

1. Introduction

Tungsten metal, which is renowned for its refractory properties such as a high melting point and remarkable hardness, has widespread utility in myriads of fields. However, the features that make it an attractive material also present challenges when processing it into thin films or complex shapes. Thus, electrodeposition has been explored as an alternative for fabricating functional tungsten films.

Tungsten is known to exist in two phases: a stable α-W with an A2 structure and a metastable β-W with an A15 structure [1]. Over the years, β-W films with the A15 structure have attracted tremendous interest, most notably in spintronic technology, as they exhibit a giant spin Hall effect [2,3]. Physical vapor deposition (PVD) has been used almost exclusively for the preparation of β-W films [2–9]. However, the PVD method is not suitable for the fabrication of thick films – the thickness of β-W films reported so far is of the order of nanometers (less than 500 nm [5]). As a result, the properties of bulk β-W, such as its spin Hall angle, hardness and elastic modulus, have not been accurately measured, and applications other than spintronics have not yet been proposed.

By contrast, electrodeposition from high-temperature molten salts, such as fluorides [10], chlorides [11–13], fluoride–chloride mixtures [14–16], and oxides [17,18], has been actively studied as a new film preparation method for the stable α-W phase. Despite the success in α-W films, the electrodeposition of β-W films remains under-explored. The first advance on this topic was the work of Katagiri et al., who obtained almost pure β-W using molten $ZnBr_2$–NaBr–WBr_5 at 723 K, although the films formed were not smooth and compact [19]. Another study by Nitta et al. also obtained mixed-phase films comprising α-W and β-W using molten Li_2WO_4–Na_2WO_4–K_2WO_4–LiCl–NaCl–KCl at 873 K [20]. In one of our recent works, we reported a relatively smooth and compact mixed-phase film obtained using molten CsF–CsCl–WO_3 at 823 K [21]. Despite these developments, there have been no reports of smooth, compact, and thick single-phase β-W films obtained through PVD or electrodeposition, to the best of our knowledge.

In this study, we employ molten CsF–CsCl–WO_3 at the lower temperature of 773 K to suppress grain growth and obtain smoother electrodeposits. Then, we obtain a thick single-phase β-W film with a mirror-like surface. Thus, we not only establish a method for obtaining desirable thick β-W films but also provide a platform for further research on the applications of β-W films.

2. Experimental

Reagent-grade CsF (Furuuchi Chemical Corp. > 99.0%) and CsCl (FUJIFILM Wako Pure Chemical Corp. > 99.0%) were first dehydrated under vacuum at 453 K for over 24 h and further dehydrated under vacuum at 773 K for 24 h. The salts were then mixed into a eutectic composition (molar ratio of CsF:CsCl = 50:50, melting point = 713 K, 150 g) and loaded into a graphite crucible which was placed at the bottom of a stainless-steel vessel. After blank measurements in molten

---

[*] Corresponding author.
E-mail address: nohira.toshiyuki.8r@kyoto-u.ac.jp (T. Nohira).

https://doi.org/10.1016/j.elecom.2021.107139
Received 14 September 2021; Received in revised form 1 October 2021; Accepted 3 October 2021

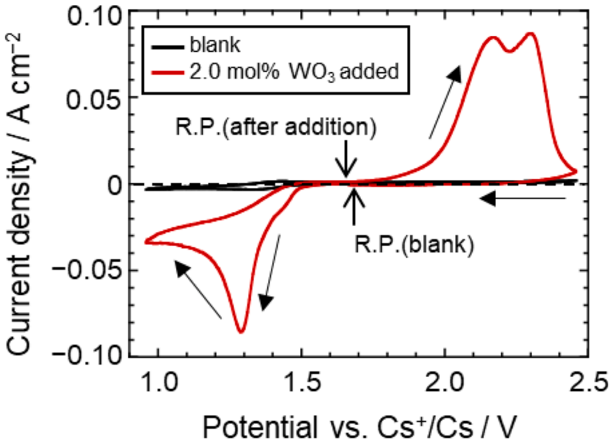

Fig. 1. Cyclic voltammograms of a Au flag electrode in a molten CsF–CsCl salt before and after addition of WO_3 (2.0 mol%) at 773 K. Scan rate: 0.2 V s^{-1}. R.P.: rest potential.

CsF–CsCl, 2.0 mol% of granular WO_3 (Kojundo Chemical Laboratory Co. Ltd., 99.9%) was directly added to the melt to act as the W(VI) ion source.

Electrochemical measurements and galvanostatic electrolysis were performed using the three-electrode method in an electrochemical measurement system (Hokuto Denko Corp., HZ-7000) under a dry Ar atmosphere. For the working electrodes, Cu foil (Nilaco Corp., thickness: 0.030, 0.05 mm, 99.9%), Ag flag (Nilaco Corp., diameter: 2.0 mm, thickness: 0.1 mm, 99.98%), and Au flag (Nilaco Corp., diameter: 2.0 mm, thickness: 0.10 mm, 99.95%) were selected. The structure of the flag electrode was reported in one of our previous works [22]. A glass-like carbon rod (Tokai Carbon Co., Ltd., diameter: 3.0 mm) and a Pt wire (Nilaco Corp., diameter: 1.0 mm, 99.98%) were employed as the counter electrode and the quasi-reference electrode, respectively. The potential of the quasi-reference electrode was calibrated with respect to the dynamic Cs$^+$/Cs potential determined by cyclic voltammetry performed on a Ag electrode. The melt temperature was measured using a type-K thermocouple. The electrolyzed samples on the Cu foils were soaked in distilled water for 10 min at 333 K to remove the salt adhering to the deposits.

Phase identification of the samples was conducted through X-ray diffractometry (XRD; Rigaku, Ultima IV, Cu-Kα, 40 kV, 40 mA). The surface and cross-sectional morphologies of the samples were investigated using scanning electron microscopy (SEM; Thermo Fisher Scientific Inc., Phenom Pro Generation 5). The surface roughness (S_a) of the samples was measured using a laser microscope (Keyence VK-X 1000). The samples were cut at the center and embedded in acrylic resin before cross-sectional SEM observations were performed. The samples were polished with emery papers and buffing compounds and subsequently coated with Au using an ion-sputtering apparatus (Hitachi Ltd., E-1010) to impart conductivity.

3. Results and discussion

To ascertain the electrochemical behavior of W, cyclic voltammetry was performed on a Au flag electrode before and after the addition of 2.0 mol% WO_3 to molten CsF–CsCl at 773 K. As shown in Fig. 1, in the absence of WO_3 (blank), almost no current is observed during the negative scan which commenced from the rest potential (1.7 V vs. Cs$^+$/Cs) to 0.95 V, as well as the proceeding positive scan, conducted up to 2.45 V. Upon the addition of WO_3, the cathodic current started to increase at around 1.50 V and formed a peak at 1.30 V during the negative scan, suggesting the reduction of W(VI) ions. When scanning was reversed to the positive direction, two anodic current peaks were observed at 2.10 V and 2.25 V – an indication that the anodic dissolution of W occurred via multi-step reaction(s). Similar observations were made in our previous study pertaining to the electrodeposition of W in molten KF–KCl–WO_3 [21]. However, this study mainly encompasses the cathodic electrodeposition of W; thus, the anodic dissolution mechanism (s) will be the subject of a future study.

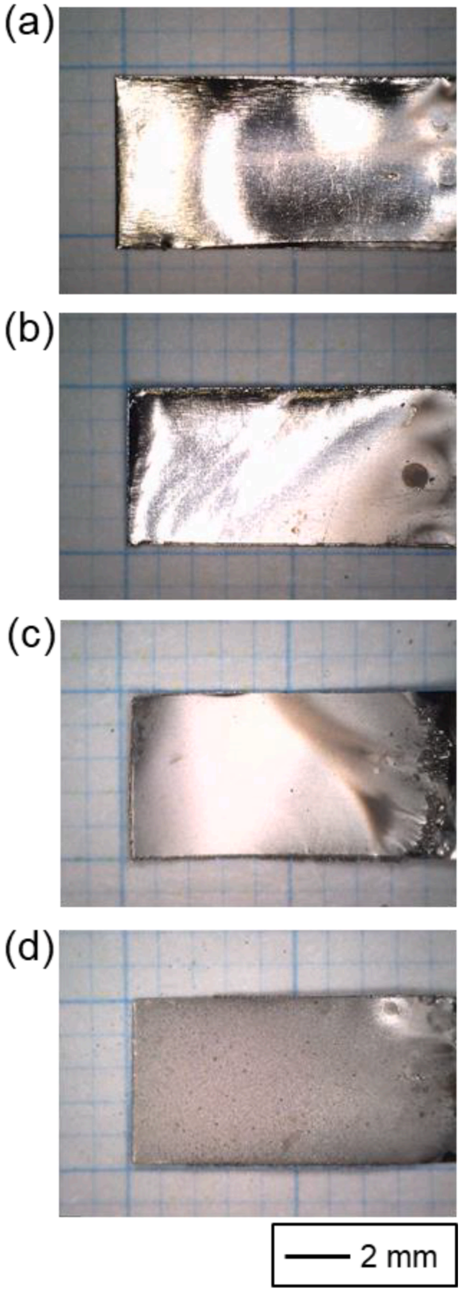

Fig. 2. Images of samples obtained through the galvanostatic electrolysis of Cu foil electrodes in the molten CsF–CsCl salt containing 2.0 mol% WO_3 at cathodic charge densities of (a) 4 mA cm^{-2}, (b) 6 mA cm^{-2}, (c) 8 mA cm^{-2}, and (d) 10 mA cm^{-2} at 773 K. Unified charge density: 90C cm^{-2}. Coating area: 5 × 10 mm.

Deposition samples were thereafter prepared through the galvanostatic electrolysis of Cu foil electrodes at 773 K at varying cathodic charge densities: (a) 4 mA cm^{-2}, (b) 6 mA cm^{-2}, (c) 8 mA cm^{-2}, and (d) 10 mA cm^{-2}. The charge density was unified to 90C cm^{-2} for comparison. Fig. 2 shows images of the various samples after washing with water. As illustrated, the samples obtained at (a) 4 mA cm^{-2} and (b) 6 mA cm^{-2} have a metallic luster, which suggests the formation of an extremely smooth surface. Remarkably, even without polishing, the

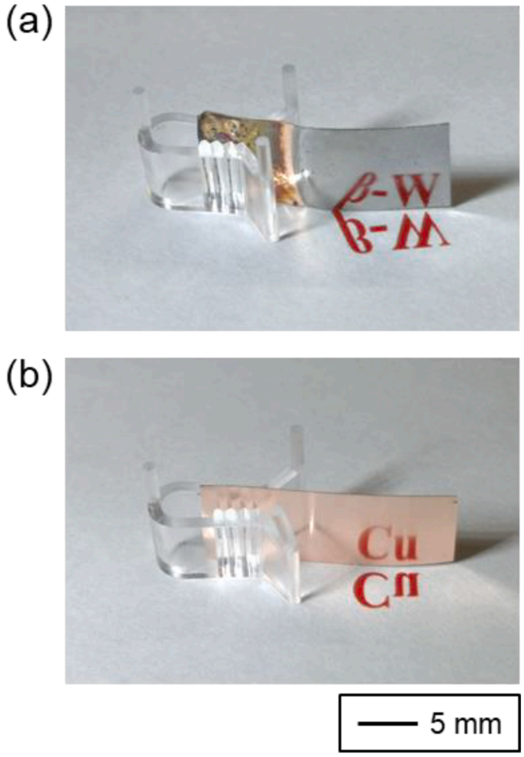

Fig. 3. Images of (a) the unpolished sample prepared by electrodeposition at a cathodic current density of 4 mA cm^{-2} and (b) an original Cu substrate. Unified charge density: 90C cm^{-2}. Coating area: 8 × 12.5 mm.

sample obtained after electrodeposition at 4 mA cm^{-2} (Fig. 3a) displays a mirror-like surface similar to that of the Cu substrate before electrodeposition (Fig. 3b).

For characterization, the obtained electrodeposition samples (shown in Fig. 2) were subjected to XRD analysis, as shown in Fig. 4. A comparison with the reference pattern (PDF #00–047-1319) confirms that all electrodeposited films are single-phase β-W. Here, it is important to note that the films obtained at (a) 4 mA cm^{-2} and (b) 6 mA cm^{-2} appear to have a strong preferred orientation along the {1 1 1} plane. To further evaluate this preferred orientation, the orientation index of the {1 1 1} plane, α_{111}, was calculated using the following formula proposed by Willson et al. [23]:

$$\alpha_{hkl} = \frac{I_{hkl}(\mathrm{sample})/\Sigma I(\mathrm{sample})}{I_{hkl}(\mathrm{PDF})/\Sigma I(\mathrm{PDF})} \quad (1)$$

Here, I_{hkl}(sample) and I_{hkl}(PDF) denote the diffraction intensities of the *hkl* indices of the deposits and the PDF data, respectively. The Σ I(sample) and ΣI(PDF) denote the sum of diffraction intensities of all *hkl* indices of the deposits and the PDF data, respectively. Subsequently, the α_{111} was plotted against the cathodic current density, as shown in Fig. 5. The plot reveals that the preferred orientation along the {1 1 1} plane of the electrodeposited β-W films becomes stronger with decreasing current densities, achieving the highest α_{111} value of 26.4 at 4 mA cm^{-2}. Considering previous work on the preferred orientations of β-W films, Hsieh et al. reported a strong preferred orientation along the {3 2 1} plane for β-W films obtained through thermal evaporation [24]. In another study by Karabacak et al., β-W nanorods obtained through oblique-angle sputter deposition manifested a preferred orientation along the {1 0 0} plane [25]. However, to date no studies on β-W films prepared by PVD have reported a preferred orientation along the {1 1 1} plane. Likewise, for electrodeposited β-W films, there is virtually no literature on preferred orientation. It is worth mentioning that previous studies have reported that the crystal orientation of electrodeposited α-W films varies depending on the current density during the galvanostatic electrolysis and the parameters in pulse electrolysis [26,27]. However, the mechanism(s) of preferred orientation are yet to be determined. In a bid to elucidate these mechanisms for β-W films, detailed analysis of samples prepared under various conditions are currently underway and will be the subject of future reports.

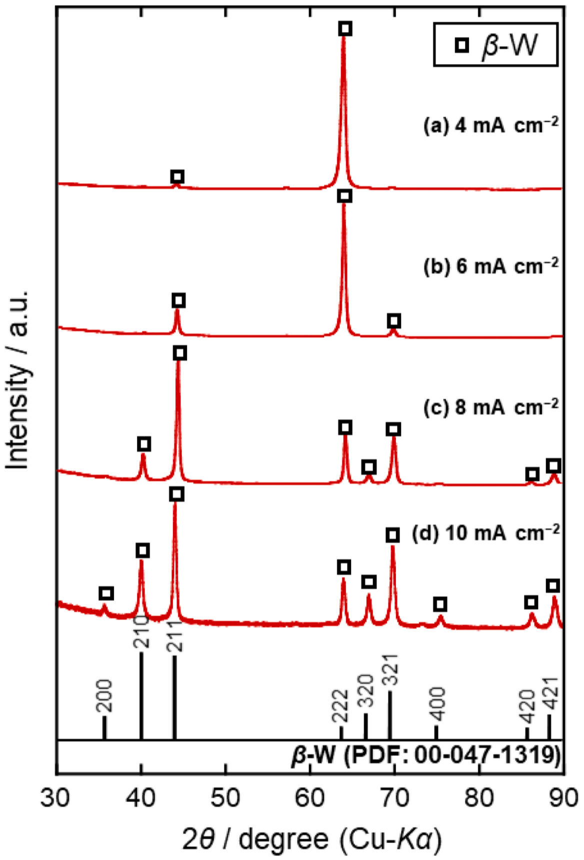

Fig. 4. XRD patterns of the samples obtained by galvanostatic electrolysis of Cu foil electrodes in the molten CsF–CsCl salt containing 2.0 mol% WO$_3$ at cathodic current densities of (a) 4 mA cm^{-2}, (b) 6 mA cm^{-2}, (c) 8 mA cm^{-2}, and (d) 10 mA cm^{-2} at 773 K. Unified charge density: 90C cm^{-2}.

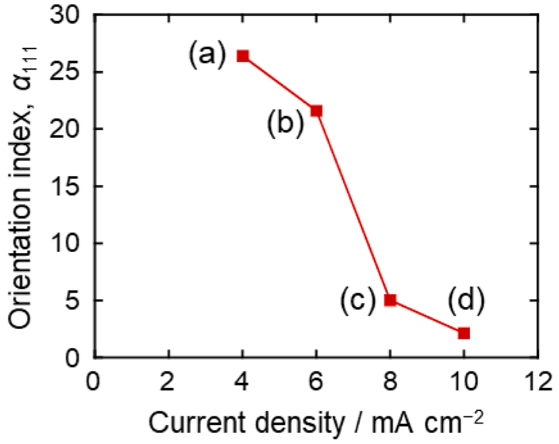

Fig. 5. Orientation indices of the {1 1 1} plane of the electrodeposited β-W films obtained at cathodic current densities of (a) 4 mA cm^{-2}, (b) 6 mA cm^{-2}, (c) 8 mA cm^{-2} and (d) 10 mA cm^{-2}. Unified charge density: 90C cm^{-2}.

To observe the morphology of the β-W film, surface and cross-sectional SEM images of the various samples were obtained as shown

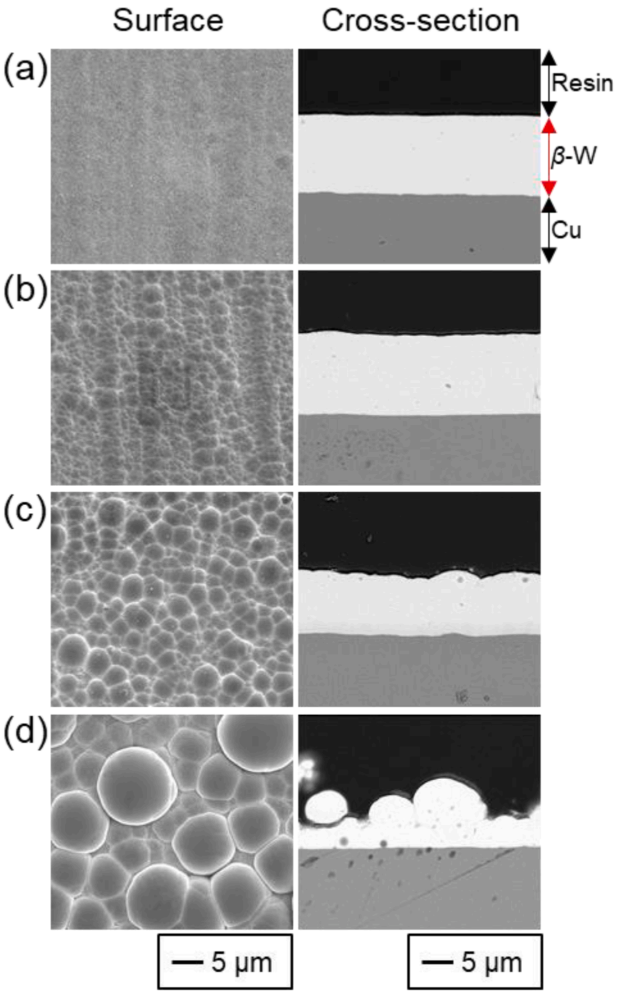

Fig. 6. Surface and cross-sectional SEM images of the β-W films obtained at cathodic current densities of (a) 4 mA cm^{-2}, (b) 6 mA cm^{-2}, (c) 8 mA cm$^{-2,}$ and (d) 10 mA cm^{-2}. Unified charge density: 90C cm^{-2}.

in Fig. 6. The sample obtained at 4 mA cm^{-2} (a) appears to be extremely smooth and flat on both the surface and its cross-section. To further evaluate the smoothness, the arithmetic mean height of the surface (S_a), which is a three-dimensional expansion of R_a, was measured with a laser microscope. A very low S_a value of 0.11 μm was obtained from the β-W film fabricated at 4 mA cm^{-2}. According to the literature describing the relationship between the surface roughness and glossiness of metals, it has been found that glossiness increases rapidly when the surface roughness (R_a) becomes smaller than 0.2 μm [28]. Since the surface roughness of the present W film was 0.11 μm (S_a), it can reasonably be classified as a mirror-like surface.

There have been several reports claiming the electrodeposition of smooth metal films (W [21,26], Ti [29,30], Nb [31], etc.) in high-temperature molten salts. However, the surface roughness (R_a) measured by a profilometer or estimated from SEM images of cross-sections were all above 0.5 μm. Therefore, the films obtained in the previous studies cannot be classified as mirror-like surfaces. As far as we know, the present study is the first time that mirror-like metal films have been electrodeposited in a high temperature molten salt, not only for tungsten but for any metal.

From the cross-sectional SEM image, the β-W film is found to have a thickness of around 13 μm. Calculations based on the weight increase determined the current efficiency to be 91%. Assuming a six-electron reaction along with the calculated current efficiency (91%), the theoretical thickness was found to be 14 μm, which is virtually equivalent to the observed thickness.

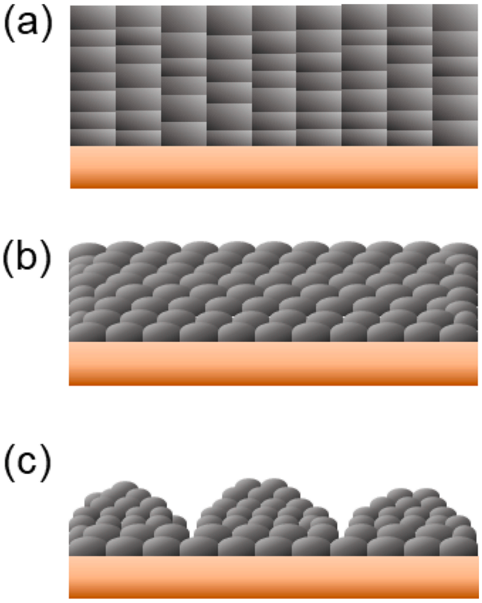

Fig. 7. Schematic diagrams showing different types of polycrystalline electrodeposit growth as proposed by Fischer [33,34]: (a) field-orientated texture (FT), (b) unoriented dispersion (UD) in coherence, and (c) unoriented dispersion (UD) in powder.

By the same token, SEM images of the samples (b)–(d) were observed, revealing the formation of larger spherical particles with increased current density, thereby diminishing the smoothness of the film surface. Using the Scherrer equation [32], the average grain crystallite size can be calculated from the XRD patterns as follows:

$$L = K\lambda/\beta cos\theta \tag{2}$$

Here, K is the shape factor (usually about 0.9), λ is the X-ray wavelength (0.154 nm for Cu-Kα), β represents the full width at half maximum of the diffraction peak, and θ is the Bragg angle. In all samples, the average size of the β-W crystallites was approximately 18–22 nm – an indication that the spherical particles are formed by a collection of fine crystallites. Here, we note that the formation of larger spherical particles at higher current densities cannot be justified by the size of the crystallites but rather can be attributed to changes in the growth type of polycrystalline electrodeposits as characterized by Fischer [33,34] (Fig. 7). Provided the metal ion concentration and inhibition intensity remain constant, relatively low current densities induce two-dimensional nucleation that forms a field-orientated texture (FT) type deposit (Fig. 7a) with smooth surfaces. At higher current densities, three-dimensional nucleation producing the unoriented dispersion (UD) type occurs, thereby forming a coherent deposit (Fig. 7b). Further increases in the current density enhance the three-dimensional nucleation, resulting in the UD powder type deposit (Fig. 7c). Although this model provides an adequate explanation for the results obtained in this study, further analysis of the metallographic structure using TEM as well as other techniques should be explored for further validation.

4. Conclusion

We report for the first time a single-phase β-W film with a mirror-like surface and a thickness of 13 μm, obtained through electrodeposition. The β-W films exhibit a preferred orientation along the {1 1 1} plane, which is noted to become stronger with decreasing current density. When the current density is increased, larger spherical particles are formed, consequently diminishing the smoothness of the film. We attribute this observation to changes in the growth of electrodeposits from FT type to UD type, in accordance with Fischer's classification of electrodeposition. Herein, we not only establish a method for obtaining thick β-W films with smooth surfaces but also provide a platform for further research on the properties of β-W films and their applications.

CRediT authorship contribution statement

Xianduo Meng: Methodology, Investigation, Data curation, Validation, Writing - original draft, Writing - review & editing. **Yutaro Norikawa:** Methodology, Validation, Writing - review & editing. **Toshiyuki Nohira:** Conceptualization, Methodology, Validation, Supervision, Writing - review & editing, Funding acquisition.

Declaration of Competing Interest

The authors declare that they have no known competing financial interests or personal relationships that could have appeared to influence the work reported in this paper.

Acknowledgement

This study was partly collaborated with Sumitomo Electric Industries, Ltd. The surface roughness was measured by Sumitomo Electric Industries, Ltd.

References

[1] H. Hartmann, F. Ebert, O. Bretschneider, Z. Anorg, Allg. Chem. 198 (1931) 116–140, https://doi.org/10.1002/zaac.19311980111.

[2] Q. Hao, W. Chen, G. Xiao, Appl. Phys. Lett. 106 (2015), 182403, https://doi.org/10.1002/zaac.19311980111.

[3] C.-F. Pai, L. Liu, Y. Li, H.W. Tseng, D.C. Ralph, R.A. Buhrman, Appl. Phys. Lett. 101 (2012), 122404, https://doi.org/10.1063/1.4753947.

[4] S.M. Rossnagel, I.C. Noyan, C. Cabral, J. Vac. Sci. Technol. B 20 (2002) 2047–2051, https://doi.org/10.1116/1.1506905.

[5] H.L. Sun, Z.X. Song, D.G. Guo, F. Ma, K.W. Xu, J. Mater. Sci. Technol. 26 (2010) 87–92, https://doi.org/10.1016/S1005-0302(10)60014-X.

[6] D. Choi, B. Wang, S. Chung, X. Liu, A. Darbal, A. Wise, N.T. Nuhfer, K. Barmak, A. P. Warren, K.R. Coffey, M.F. Toney, Phase, J. Vac. Sci. Technol. A 29 (2011), 051512, https://doi.org/10.1116/1.3622619.

[7] Q. Hao, G. Xiao, Phys. Rev. Appl. 3 (2015), 034009, https://doi.org/10.1103/PhysRevApplied.3.034009.

[8] J.-S. Lee, J. Cho, C.-Y. You, J. Vac. Sci. Technol. A 34 (2016), 021502, https://doi.org/10.1116/1.4936261.

[9] S. Mondal, S. Choudhury, N. Jha, A. Ganguly, J. Sinha, A. Barman, Phys. Rev. B 96 (2017), 054414, https://doi.org/10.1103/PhysRevB.96.054414.

[10] S. Senderoff, G.W. Mellors, Science 153 (1966) 1475–1481, https://doi.org/10.1126/science.153.3743.1475.

[11] K. Nitta, S. Inazawa, K. Okada, H. Nakajima, T. Nohira, R. Hagiwara, Electrochim. Acta 53 (2007) 20–23, https://doi.org/10.1016/j.electacta.2007.01.032.

[12] H. Takenishi, A. Katagiri, Electrochemistry 67 (1999) 669–676, https://doi.org/10.5796/electrochemistry.67.669.

[13] R. Abdulaziz, L.D. Brown, D. Inman, S. Simons, P.R. Shearing, D.J.L. Brett, Electrochem. Comm. 41 (2014) 44–46, https://doi.org/10.1016/j.elecom.2014.01.022.

[14] H. Nakajima, T. Nohira, R. Hagiwara, K. Nitta, S. Inazawa, K. Okada, Electrochim. Acta 53 (2007) 24–27, https://doi.org/10.1016/j.electacta.2007.04.082.

[15] Y. Qi, Y. Tang, B. Wang, M. Zhang, X. Ren, Y. Li, Y. Ma, Int. J. Refract. Met. Hard Mater. 81 (2019) 183–188, https://doi.org/10.1016/j.ijrmhm.2019.03.006.

[16] K. Nitta, T. Nohira, R. Hagiwara, M. Majima, S. Inazawa, Electrochim. Acta 55 (2010) 1278–1281, https://doi.org/10.1016/j.electacta.2009.10.021.

[17] F. Jiang, Y. Zhang, N. Sun, J. Leng, Appl. Surf. Sci. 327 (2015) 432–436, https://doi.org/10.1016/j.apsusc.2014.11.186.

[18] K. Koyama, M. Morishita, T. Umezu, Electrochemistry 67 (1999) 677–683, https://doi.org/10.5796/electrochemistry.67.677.

[19] A. Katagiri, M. Suzuki, Z.i. Takehara, J. Electrochem. Soc. 138 (1991) 767–773, https://doi.org/10.1149/1.2085673.

[20] K. Nitta, M. Majima, S. Inazawa, T. Nohira, R. Hagiwara, Electrochemistry 77 (2009) 621–623, https://doi.org/10.5796/electrochemistry.77.621.

[21] T. Nohira, T. Ide, X. Meng, Y. Norikawa, K. Yasuda, J. Electrochem. Soc. 168 (2021), 046505, https://doi.org/10.1149/1945-7111/abf266.

[22] K. Maeda, K. Yasuda, T. Nohira, R. Hagiwara, T. Homma, J. Electrochem. Soc. 162 (2015) D444–D448, https://doi.org/10.1149/2.0441509jes.

[23] K.S. Willson, J.A. Rogers, Tech. Proc. Am. Electroplaters Soc. 51 (1964) 92.

[24] C.-T. Hsieh, J.-M. Ting, J. Vac. Sci. Technol. A 25 (2007) 1552–1556, https://doi.org/10.1116/1.2790913.

[25] Tansel Karabacak, Anupama Mallikarjunan, Jitendra P. Singh, Dexian Ye, Gwo-Ching Wang, Toh-Ming Lu, β-Phase tungsten nanorod formation by oblique-angle sputter deposition, Appl. Phys. Lett. 83 (15) (2003) 3096–3098, https://doi.org/10.1063/1.1618944.

[26] F. Jiang, Y. Zhang, N. Sun, Z. Liu, Appl. Surf. Sci. 317 (2014) 867–874, https://doi.org/10.1016/j.apsusc.2014.09.031.

[27] X.-Q. Fang, Y. Zhang, K.-G. Zhu, W.-J. Han, J.-G. Yu, Z. Chen, H.-J. Shi, Rare Metals 37 (2016) 407–412, https://doi.org/10.1007/s12598-016-0825-1.

[28] M. Yonehara, T. Matsui, K. Kihara, Hi. Isono, A. Kijima, T. Sugibayashi, Mater. Trans. 45 (2004) 1027–1032, https://doi.org/10.2320/matertrans.45.1027.

[29] A. Robin, R.B. Ribeiro, J. Appl. Electrochem. 30 (2000) 239–246, https://doi.org/10.1023/A:1003994100902.

[30] Y. Norikawa, K. Yasuda, T. Nohira, J. Electrochem. Soc. 166 (2019) D755–D759, https://doi.org/10.1149/2.1291914jes.

[31] P. Chamelot, P. Taxil, D. Oquad, J. Serp, B. Lafage, J. Electrochem. Soc. 147 (2000) 4131–4137, https://doi.org/10.1149/1.1394030.

[32] A.L. Patterson, Phys. Rev. 56 (1939) 978–982, https://doi.org/10.1103/PhysRev.56.978.

[33] H. Fischer, Elektrolytische Abscheidung und Elektrokristallisation von Metallen, Springer Verlag Berlin, 1954, 10.1007/978-3-642-86549-7.

[34] R. Winand, Electrochim. Acta 39 (1994) 1091–1105, https://doi.org/10.1016/0013-4686(94)E0023-S.